Journal of Luminescence 178 (2016) 234–240

Contents lists available at ScienceDirect

Journal of Luminescence

journal homepage: www.elsevier.com/locate/jlumin

Full Length Article

Red luminescence of Zn /ZnO core–shell nanorods in a mixture of LTZA/Zinc acetate matrix: Study of the effects of Nitrogen bubbling, Cobalt doping and thioglycolic acid

Masoud Karimipour*, Alireza Kheshabnia, Mehdi Molaei

Department of Physics, Faculty of Science, Vali-E-Asr University, Rafsanjan, Iran

ARTICLE INFO

Article history:
Received 18 December 2015
Received in revised form
8 May 2016
Accepted 1 June 2016
Available online 6 June 2016

Keywords:
Zn/ZnO core–shells
Photoluminescence
Thioglycolic acid
Gas bubbling
Doping

ABSTRACT

Zn/ZnO core–shell nanorods were synthesized using a very simple low temperature and low pressure Solvothermal method. Effect of N_2 gas bubbling, insertion of thioglycolic acid (TGA) and cobalt doping with $Co/Zn=x$: 0%, 0.1%, 0.3% and 0.5% was studied by means of scanning electron microscopy, transmission electron microscopy, x-ray diffraction, Furrier transformed infrared(FTIR) spectroscopy, UV–Vis spectroscopy and photoluminescence (PL) measurement. XRD analysis showed that hexagonal metallic zinc and wurtzite ZnO phases are available in all the samples. Zinc acetate crystallizes together with Zn and ZnO phases as well, but it transforms to l-thereonine zinc acetate(LTZA) after the insertion of TGA. Moreover, gas bubbling and cobalt doping do not change the crystal phases. FTIR spectroscopy also confirms the formation of zincacetate and LTZA phases. Williamson–Hall analysis indicates that with the insertion of TGA, mean crystallite size decreases and the value of microstrain is the least for $x=0.1\%$. SEM images depict that with the insertion of TGA, the morphology of the compound changes from rounded particles to nanorods. TEM images revealed that the microstructure of the compounds is of the Zn/ZnO core–shell type. UV–vis spectroscopy demonstrates the blue shift of absorption edge and the size reduction due to insertion of TGA. PL spectroscopy shows that the samples have strong blue emission with peaks range from 316 nm up to 480 nm. Bubbling simply causes that the samples emit a narrow and sharp band peaked at 605 nm. Insertion of TGA prevents the blue emission and enhances the pure red emission band. At the presence of TGA, the optimum value of pure red emission for Co-doping was found to be 0.1% which was compatible with XRD analysis. With $x>0.1\%$, the blue and red emission of samples started quenching and light emission for the value of $x=0.5\%$ vanished completely. The results show that the other crystal phases such as zincacetate, LTZA do not affect the luminescence of the samples. It is suggested that N_2 gas bubbling accompanied by the growth of Zn/ZnO core–shells gives rise to a dramatic increase of the number of deep levels at the interface of metal/semiconductor. This would cause the appearance of a narrow red emission at room temperature. TGA insertion successfully incorporated as new capping agent for the enhancement of ZnO emission.

1. Introduction

ZnO nanostructures have been widely studied due to their versatile applications. Especially their luminescence properties have been extensively studied due to their application for light emitting diodes (LEDs) and laser fabrication [1–13]. Room temperature visible emission of ZnO nanostructures from blue to red wavelengths has been reported by many groups [8–27]. The green, yellow and red light emissions which are attributed to the deep level emission bands have previously been attributed to several defects in the ZnO crystal structure, e.g. O vacancy (V_O) [13] Zn vacancy (V_{Zn}) [14], O interstitial (O_i) [15] and Zn interstitial (Zn_i) [16,17]. The key role in the luminescence properties of ZnO nanostructures have been realized to be defect engineering [8,17–27]. The defects have been extensively manipulated by insertion of doping agents into the ZnO crystal structure. Different groups have reported green to red emission of ZnO by insertion of Copper (Cu), Manganese (Mn) and Europium (Eu) as doping agent in the structure of ZnO [19–22]. The luminescence modification of ZnO nanorods (NRs) doped with arsenic (As) [23], Cu [24] phosphorus (P) [25], antimony (Sb) [26] and nitrogen (N) [27] have been published and the effect of introducing these elements on the luminescent properties was investigated. The origin of the red

---

* Corresponding author at: Assistant Professor of Physics, Department of Physics, Vali-E-Asr University of Rafsanjan, Rafsanjan, Iran. Tel.: +989352262987; fax: +983431312429.
E-mail address: masoud.karimipour@gmail.com (M. Karimipour).

http://dx.doi.org/10.1016/j.jlumin.2016.06.003
0022-2313/© 2016 Elsevier B.V. All rights reserved.

emission peaks is attributed to the electron transition from deep level defects such as oxygen vacancies and oxygen interstitials to valence band (VB), usually observed in the oxygen rich systems and Eu-doped ZnO nanostructures [28]. According to different reports, this red emission is broad and weak at room temperature [22,28,29]. Some other reports refer to the surface modification of ZnO nanostructures in the presence of polymers or capping agents. For example, Yan et al. have increased the quantum yield of ZnO based LEDs using poly (9,9-dioctyl-fluorene-co-N(4-butylphenyl) diphenylamine) (TFB-PVK) polymer [30]. Alvi et al. have obtained red emission from ZnO nanotubes grown on GaN nanorods [31,32]. Moreover, new featured Zn/ZnO nanostructures have been a new era of investigation due to the unique properties of metal/semiconductor interface [33,34]. The capability of creation of highly defective structures at the interface of Zn@ZnO core–shells resulted in a broad but strong emission of visible light rather than UV light emission according to Jin-Han et al. [34]. They attributed the higher intensity of visible emission than UV emission to the nature of defective metal/semiconductor interface [34]. Recently, thioglycolic acid (TGA) has been widely used as capping agent for the synthesis of different quantum dots (QDs) in aqueous media. Its main functionality is to control the particle growth and passivates surface defects to enhance luminescence properties of QDs [35–37]. In this work we observed a narrow red light emission from Co doped Zn/ZnO core–shell nanorods using gas bubbling and TGA.

2. Experimental method

Cobalt doped Zn/ZnO core–shell nanorods were prepared by a similar apparatus which has been reported in our recent reports [8,38]. Firstly, a stock solution of cobalt precursor was prepared with solving 0.01 g $Co(NO_3)_2.2H_2O$ in 5 ml ethanol. Secondly, 0.1 g Zinc acetate ($Zn(CH_3COO)_2 2H_2O$) was dissolved in 50 ml ethanol (96%). Then an amount of the stoke of cobalt source containing Co/Zn:x: 0%, 0.1%, 0.3%, 0.5% was injected subsequently to the zinc solution and acetic acid was drop wise added to it until the solution became clear. Thirdly, thioglycolic acid (TGA: 1 M) was injected to the prepared solution and 2 ml NH_4OH was added drop wise and stirred vigorously to make a clear solution. The resultant clear solution was transferred to a three neck rounded bottom flux (depicted in Ref. [36]) and N_2 flow was passed through the solution with the rate of 1 ml/s at room temperature for 0, 0.5 and 1 h. Thereafter, the flux was sealed with N_2 gas and kept between 75–80 °C for 1 h. The precipitated powder was collected each time and washed with ethanol for further analysis. Table 1 shows the experimental parameters of the prepared samples.

X-ray diffraction (XRD) was performed using an advanced d8-Bruker system. Optical absorption and photoluminescence (PL) measurements were performed using an Avantes spectrometer (AvaSpec-2048 TEC). SEM images have been obtained using LEO 1450 VP system. Transmission electron microscope (TEM) images were taken by a Philips EM 208 transmission electron microscope with an accelerating voltage of 100 kV. Furrier transformed infrared (FTIR) data were collected using an AVATAR-370-FTIR THERMONICOLET spectrometer using two separate procedures. The sample was unpacked into a tablet shape and put onto a polished silicon wafer before analysis.

Table 1
Experimental sample parameters.

Sample	Bubbling time (h)	TGA (µl)	x=Co/Zn (%)
Reference	0	0	0
S0	1	0	0
S1	1	0	0.1
S2	1	500	0.1
S3	1	1000	0.1
S4	1	1000	0.3
S5	1	1000	0.5
S6	1	1000	0
S7	0.5	1000	0.1
S8	0	1000	0.1

3. Results and discussion

The experimental procedure has been performed with the consideration of three parameters: variation of Nitrogen sparging time, TGA insertion and Cobalt doping variation (x: 0, 0.1%, 0.3%, 0.5%). The analysis of the experiments has been studied based on mentioned parameters.

3.1. Structural characterization

Fig. 1 depicts XRD pattern of samples with different TGA for the fixed bubbling time of 1 h and x=0.1%. The Reference and S0 (Table 1) have the same pattern as S1 but not shown here. The sample without TGA (S1) contains the zinc acetate phase with Bragg peaks at 2θ=11.84, 18.55, 19.45, 24.20, 21.08, 22.29, 33.16, 35.70, 37.45, 39.63 and 40.82° [39]. the peak at 2θ=34.4° is attributed to (002) plane of wurtzite phase of ZnO [33,34,40,41]. The Bragg reflections at 2θ=17.7°, 30.9°, 35.3°, 36.9°, 39.9°, 44.3° and 45.9° could be indexed to the (1 0 0), (1 1 0), (1 1 2), (2 0 1), (2 0 2), (2 0 3) and (1 0 5) planes of the hexagonal phase of Zn (JCPDS: 01-1238, space group: P63/mmc), respectively [33,34,41,42]. With the insertion of TGA, the crystal structure changes dramatically and new phases of L-theorenine, L-threonine zinc acetate (LTZA) have been observed [39]. The details of peak indices and Bragg angles of L-theorenine and LTZA are discussed in Ref. [37]. Fiffraction peaks at 2θ=31.7°, 34.4°, 47.5°,56.5°, 62.8°, 66.3°, 67.9°, 69.0°, 72.5° and 76.9° (Fig. 1-inset), which could be indexed to the (1 0 0), (0 0 2), (1 0 2), (1 1 0),(1 0 3), (2 0 0), (1 1 2), (2 0 1), (0 0 4) and (2 0 2) planes of pure ZnO in a hexagonal phase (JCPDS: 80-0075, space group: P63mc), respectively [34,40]. To investigate the effect of TGA insertion on the structural properties, Williamson–Hall analysis was employed to calculate the mean crystallite size and microstrain using the following equation [40]:

$$\beta \cos(\theta) = K\lambda/D + 4\epsilon \sin(\theta) \quad (1)$$

where, β is FWHM, λ is the wavelength and θ is the Bragg angle, D

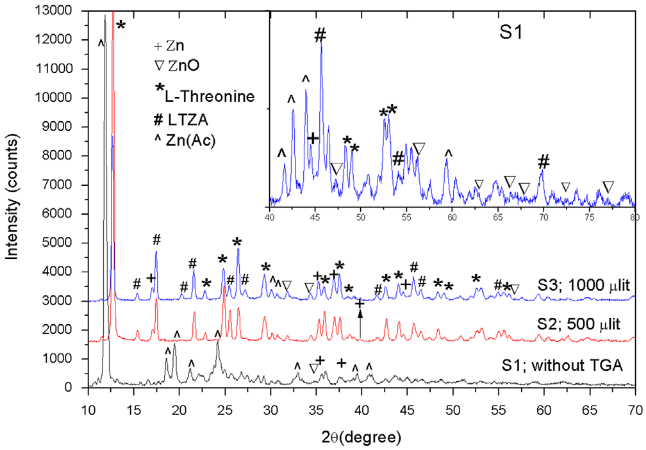

Fig. 1. XRD pattern of the samples for different TGA values with the fixed time of 1 h bubbling and x=0.1% (inset: XRD pattern of S1).